Photoprotective qH occurs in the light-harvesting complex II trimer

Pierrick Bru[a,1], Collin J. Steen[b,c,d,1], Soomin Park[b,c,d,1], Cynthia L. Amstutz[e], Emily J. Sylak-Glassman[b,c,d], Michelle Leuenberger[b,c,d], Lam Lam[c,d,f], Fiamma Longoni[g], Graham R. Fleming[b,c,d,f], Krishna K. Niyogi[c,e], Alizée Malnoë[a]*

[a]Umeå Plant Science Centre (UPSC), Department of Plant Physiology, Umeå University, 901 87 Umeå, Sweden
[b]Department of Chemistry, University of California, Berkeley, CA 94720
[c]Molecular Biophysics and Integrated Bioimaging Division, Lawrence Berkeley National Laboratory, Berkeley, CA 94720
[d]Kavli Energy Nanoscience Institute, Berkeley, CA 94720
[e]Howard Hughes Medical Institute, Department of Plant and Microbial Biology, University of California, Berkeley, CA 94720
[f]Graduate Group in Biophysics, University of California, Berkeley, CA 94720
[g]Institute of Biology, University of Neuchâtel, 2000 Neuchâtel, Switzerland

[1]These authors contributed equally to this work

*Correspondence to: alizee.malnoe@umu.se

Keywords: energy dissipation; non-photochemical quenching qH; *Arabidopsis thaliana*; light-harvesting complexes; chlorophyll fluorescence lifetime

Abstract

Excess light can induce photodamage to the photosynthetic machinery, therefore plants have evolved photoprotective mechanisms such as non-photochemical quenching (NPQ). Different NPQ components have been identified and classified based on their relaxation kinetics and molecular players. The NPQ component qE is induced and relaxed rapidly (seconds to minutes), whereas the NPQ component qH is induced and relaxed slowly (hours or longer). Molecular players regulating qH have recently been uncovered, but the photophysical mechanism of qH and its location in the photosynthetic membrane have not been determined. Using time-correlated single-photon counting analysis of the *Arabidopsis thaliana* suppressor of quenching 1 mutant (*soq1*), which displays higher qH than the wild type, we observed shorter average lifetime of chlorophyll fluorescence in leaves and thylakoids relative to wild type. Comparison of isolated photosynthetic complexes from plants in which qH was turned ON or OFF revealed a chlorophyll fluorescence decrease specifically in the trimeric light-harvesting complex II (LHCII) fraction when qH was ON. LHCII trimers are composed of Lhcb1, 2 and 3 proteins, so CRISPR-Cas9 edited and T-DNA insertion *lhcb1, lhcb2* and *lhcb3* mutants were crossed with *soq1*. In *soq1 lhcb1*, *soq1 lhcb2*, and *soq1 lhcb3*, qH was not abolished, indicating that no single major Lhcb isoform is necessary for qH. Using transient absorption spectroscopy of isolated thylakoids, no spectral signatures for chlorophyll-carotenoid excitation energy quenching or charge transfer quenching were observed, suggesting that qH may occur through chlorophyll-chlorophyll excitonic interaction.

Introduction

Photosynthetic organisms possess pigment-protein antenna complexes, which can switch from a light-harvesting state to an energy-dissipating state (1, 2). This switching capability regulates how much light is directed towards photochemistry and ultimately how much carbon dioxide is fixed by photosynthesis (3). The fine-tuning of light energy usage is achieved at the molecular level by proteins which act at or around these pigment-protein complexes (4). Understanding the regulatory mechanisms involved in the protection against excess light, or photoprotection, has important

implications for engineering optimized light-use efficiency in plants, and thereby increasing crop productivity and/or tolerance to photooxidative stress (5-7).

Non-photochemical quenching (NPQ) processes protect photosynthetic organisms by safely dissipating excess absorbed light energy as heat (8, 9). Several NPQ mechanisms have been described and classified based on their recovery kinetics and/or molecular players involved (10-12). In plants, the rapidly reversible NPQ, qE, relies on ΔpH, the protein PsbS, and the carotenoid pigment zeaxanthin (13). The slowly reversible NPQ, or sustained energy dissipation, includes several mechanisms such as qZ (zeaxanthin-dependent, ΔpH-independent (14)), qH (see below), and qI (D1 photoinactivation (15)). We have recently uncovered, using chemical mutagenesis and genetic screens in *Arabidopsis thaliana*, several molecular players regulating qH (16-19). qH requires the plastid lipocalin, LCNP (17), is negatively regulated by suppressor of quenching 1, SOQ1 (16), and is turned OFF by relaxation of qH 1, ROQH1 (18). Strikingly, when qH is constitutively ON in a *soq1 roqh1* mutant, plants are severely light-limited and display a stunted phenotype (18). If qH cannot occur (as in an *lcnp* mutant), a higher amount of lipid peroxidation is observed, and plants are severely light-damaged under stress conditions such as cold temperature and high light (17, 20). Our present working hypothesis is that, under stress conditions, LCNP binds or modifies a molecule in the vicinity of or within the antenna proteins, thereby triggering a conformational change that converts antenna proteins from a light-harvesting to a dissipative state.

In wild-type (WT) *Arabidopsis* plants, qH occurs in response to cold and high light (17), whereas the *soq1* mutant can display qH under non-stress conditions upon a 10-min high light treatment (16). In the double mutant *soq1 chlorina1,* in which the antenna of photosystem II (PSII) does not accumulate, qH is no longer observed, suggesting that qH occurs in the peripheral antenna of PSII (17). Here, we aimed to investigate the photophysical mechanism of qH and narrow down the location of the qH quenching site within the peripheral antenna of PSII. Possible photophysical mechanisms are chlorophyll (Chl)-carotenoid (Car) energy transfer (21-24), Chl-Car charge-transfer (25-28), and/or Chl-Chl charge transfer (29); these possibilities were reviewed recently for qE (30). The spectral signatures of Chl-Car species can be obtained using ultrafast spectroscopy on isolated thylakoid membranes or pigment-protein complexes. In plants, the peripheral antenna of PSII is composed of pigment-binding, light-harvesting complex (Lhcb) proteins, which are divided into minor subunits (Lhcb4, 5, 6 or CP29, 26, 24, respectively) present as monomers and major

subunits (Lhcb1, 2, 3) also referred to as LHCII, forming hetero- and homo-trimeric complexes associated to PSII in a strongly, moderately or loosely bound manner (31, 32). The pigments associated with the major and minor antenna complexes include chlorophylls *a* and *b*, and carotenoids such as lutein, violaxanthin, zeaxanthin, and neoxanthin (33).

We measured the Chl fluorescence lifetimes of intact leaves, isolated thylakoids, and isolated antenna complexes from various *Arabidopsis* mutants relating to qH under non-stress and stress conditions with qH ON or OFF. We also probed for potential Chl-Car species formed when qH is ON. Due to the sustained nature of qH, we were able to isolate antenna complexes that remained quenched after purification. This approach showed that qH occurs in the major trimeric LHCII complexes. Through genome editing and genetic crosses, we further demonstrated that qH does not however rely on a specific major Lhcb subunit, suggesting that compensation from other major Lhcb proteins may occur.

Results

Fluorescence lifetimes from leaves are shorter with qH ON

We have previously found that the amount of NPQ measured by chlorophyll fluorescence imaging can reach a high level (approximately 12 in the *soq1* mutant) when qH is induced by a cold and high light treatment on whole plants of *Arabidopsis*, but the induction of qH is prevented in a *soq1 lcnp* double mutant (17). Furthermore, the maximum fluorescence (F_m) from dark-acclimated *soq1 roqh1* plants that display constitutive qH is much lower than control (41 ± 6 in the *soq1 roqh1* mutant vs. 272 ± 8 in wild type), indicating a high NPQ yield, and this quenching does not occur in a *soq1 roqh1 lcnp* triple mutant (18). To confirm these findings, we used time-correlated single-photon counting (TCSPC) to measure the fluorescence lifetime from intact leaves (34) of *soq1*, *soq1 roqh1 lcnp* (as a negative control that lacks qH), wild type, and *soq1 roqh1*. The amplitude-weighted average fluorescence lifetimes (τ_{avg}) of these first three genotypes were similar in dark-acclimated plants (~1.5 ns, Fig. 1), whereas *soq1 roqh1* displayed a much shorter value (~0.1 ns) consistent with constitutive qH described in (18).

To induce qH in wild type and *soq1*, we exposed the plants to a 6-h cold and high light treatment. During this treatment, qH is induced and so is qZ as zeaxanthin accumulates (de-epoxidation state value of approximately 0.7 (stress) vs. 0.05 (non-stress) in all lines (17, 18)); the

remaining slowly relaxing quenching processes are grouped under the term qI and are in part due to photoinactivation of PSII. The average fluorescence lifetime of *soq1* cold and high light treated leaves reached similar values as *soq1 roqh1* dark-acclimated leaves (Fig. 1, Fig. S1 and Table S1). Importantly, the calculated NPQτ derived from the τ_{avg} values in *soq1* was approximately 11, which is comparable with the NPQ value measured by video imaging of pulse-amplitude modulated chlorophyll fluorescence. We also observed a lower τ_{avg} value for wild type compared to *soq1 roqh1 lcnp*, consistent with the requirement of LCNP for qH and the induction of qH in wild type by the combination of cold and high light.

Fluorescence lifetimes from isolated thylakoids are shorter with qH ON

Next, we measured fluorescence lifetimes from isolated thylakoids. Isolated thylakoids from dark-acclimated wild type, *soq1*, and *soq1 roqh1 lcnp* displayed similar τ_{avg} (~1.1 ns, Fig. 2, grey bars), and isolated thylakoids from dark-acclimated *soq1 roqh1* displayed a much lower value (~0.2 ns) consistent with the observations in Fig. 1. Thylakoids were then isolated from plants exposed to a 6-h cold and high light treatment, followed by dark-acclimation for 5 min to relax qE. After a cold and high light treatment, *soq1* also displayed the shortest τ_{avg} of the three lines treated (~0.4 ns vs. ~0.6 ns, Fig. 2), but those values were all higher than what was observed in intact leaves, and the difference in τ_{avg} between wild type and *soq1 roqh1 lcnp* was no longer apparent. The calculated NPQ derived from τ_{avg} was therefore lower than what we observed in intact leaves, but nevertheless the slow relaxation of qH enabled us to measure a difference in NPQτ (2 in *soq1* vs. 0.7 in wild type and *soq1 roqh1 lcnp*) even after the 2 h needed for thylakoid isolation. Release of chlorophyll fluorescence by step solubilization of thylakoid membrane preparation showed that qH depends on incorporation of pigment-protein complexes in the thylakoid (Fig. S2, Q_m *soq1* higher than *soq1 roqh1 lcnp*) and into chlorophyll–protein complexes (Q_{Pi}).

qH is observed in isolated major LHCII

Next, we tested whether we could measure qH from isolated pigment-protein complexes. The lines *soq1* (with qH ON) and *soq1 lcnp* (with qH OFF) were treated with cold and high light (the *roqh1* mutation was omitted as the lack of qH-phenotype remains in either *soq1 roqh1 lcnp* or *soq1 lcnp*), and thylakoids were isolated, solubilized, and fractionated by gel filtration to separate complexes

based on their size. The separation profiles of photosynthetic complexes were similar for *soq1* and *soq1 lcnp* (Fig. S3). Fractions corresponding to PSII-LHCII mega-complexes, supercomplexes, PSI-LHCI supercomplexes, PSII core dimer, LHCII trimer, and LHCII monomer as well as smaller fractions (peaks 7, 8) were collected, and their fluorescence yield was measured by video imaging. The LHCII trimer fraction clearly displayed a relatively lower fluorescence value with qH ON (Fig. S4). Room-temperature fluorescence spectra were measured at same low Chl concentration (0.1 μg mL^{-1}) to prevent re-absorption and with excitation at 625 nm (isosbestic point) to excite both Chls *a* and *b* equally. Complexes from untreated WT were isolated for reference. The LHCII trimer fraction displayed a fluorescence yield at 680 nm that was 20% lower when qH was ON compared to qH OFF and WT reference (Fig. 3A), whereas the LHCII monomer fraction displayed no differences among samples (Fig. 3B). This result suggests that qH occurs specifically in the LHCII trimer and can be measured even after isolation of the solubilized protein complex. We confirmed by immunoblot analysis that the protein composition of the compared fractions is similar, namely the LHCII trimer fraction from qH ON and OFF similarly contains a high amount of Lhcb2 and a low amount of Lhcb4 (Fig. S5). We observed a higher content of Lhcb2 in the monomer fractions from the cold and high light treated samples compared to untreated wild type, which could be due to monomerization of trimers during the cold and high light treatment. A complementary approach separating pigment-protein complexes following solubilization by clear native-PAGE confirmed that qH is evident in isolated LHCII trimers (Fig. 4).

Fluorescence lifetimes from isolated LHCII trimer are shorter with qH ON

To further characterize the difference in fluorescence yield observed only from isolated LHCII trimers with qH ON and OFF, we measured their Chl fluorescence lifetimes. Consistent with the 20% decrease in yield, we observed in the LHCII trimer fraction a 20% shorter τ_{avg} with qH ON (~2.6 ns, Fig. 5, red bar) vs. qH OFF (~3.3 ns, Fig. 5, blue bar) and no differences in lifetimes in the LHCII monomer and PSII core dimer fractions (red and blue bars). Interestingly, the τ_{avg} from cold and HL-treated LHCII trimer with qH OFF was not significantly different from untreated wild type, and in contrast, the LHCII monomer fractions from cold and HL-treated samples displayed shorter lifetimes compared to untreated wild type. This difference could be attributable to qZ (14) that is present in the cold and HL-treated samples irrespective of LCNP presence, as both qH ON

and OFF monomer samples display the same shorter lifetimes compared to untreated wild type monomer.

We examined the pigment and protein content by HPLC and SDS-PAGE, respectively, in the LHCII trimer fractions with qH ON or OFF. There were no apparent differences in pigment composition (Fig. S6) or abundance (Fig. S7). This result is in agreement with previous genetic dissection of qH, which did not find involvement of violaxanthin, zeaxanthin, or lutein (16, 17). The protein content was also similar, and there were no visible additional protein bands or size shifts (Fig. S8).

qH does not rely on a specific major Lhcb subunit

As a parallel approach to narrow down the antenna site for qH, we used genetic crosses to combine the *soq1* mutation with *lhcb* mutations. The expectation is that the enhanced qH in the *soq1* mutant would no longer be observed if its Lhcb quenching site is absent. We crossed the *soq1* mutant to *lhcb1* and *lhcb2* mutant lines generated by CRISPR-Cas9 genome editing and to the T-DNA insertional mutant *lhcb3*. The dissection of the Lhcb quenching site is complicated because there are five *LHCB1* and three *LHCB2* genes. However *LHCB1.1, 1.2,* and *1.3* are neighboring genes, as well as *LHCB1.4* and *1.5*, so only three "loci" are segregating upon generating the sextuple mutant *soq1 lhcb1*. The situation is similar for the quadruple *soq1 lhcb2* mutant with three "loci" segregating: *SOQ1*, *LHCB2.1* and *2.2*, and *LHCB2.3*. In addition to genotyping by PCR, lack of specific Lhcb isoforms was confirmed by immunoblot analysis (Fig. S9). In all three mutant combinations, *soq1 lhcb1*, *soq1 lhcb2*, or *soq1 lhcb3*, additional quenching compared to the respective *lhcb* mutant controls was observed (Fig. 6), which suggests that qH does not require a specific Lhcb isoform.

No CT or S1 signatures were observed with qH ON

We used transient absorption (TA) spectroscopy to monitor the signatures of charge transfer (CT) (27) or excitation energy transfer (EET) (22) quenching mechanisms in isolated thylakoids. There was no difference between *soq1* (qH ON) and *soq1 roqh1 lcnp* (qH OFF) thylakoids: no detectable Car S_1 (Fig. 7) or $Car^{\bullet+}$ (Fig. 8) excited state absorption following Chl excitation. Having qH ON does not appear to affect the excitation energy populations in CT and Car S1 states, which implies

that Chl-Car EET and CT mechanisms may not be involved in qH. The absence of an observable EET or CT signal does not exclude their involvement in qH; it is possible that the low overall magnitude of NPQ from *Arabidopsis* thylakoids contributes to the inability to observe a TA signal.

Discussion

In this paper, we sought to determine the photophysical mechanism of qH and its location within the peripheral antenna of PSII. We found that qH does not seem to rely on either Chl-Car energy or charge transfer mechanisms (Fig. 7, 8), and it does not require a specific Lhcb component of LHCII trimers (Fig. 6). Fluorescence lifetimes of isolated trimer fractions indicate that qH likely occurs in the trimeric LHCII (Fig. 5), but the native thylakoid environment is required for its full extent of quenching (Fig. 1). An alternative explanation could be that qH relaxes slowly during isolation of thylakoids or photosynthetic complexes.

Potential quenching mechanism

Based on the enhanced qH phenotype remaining in the different genetic combinations of *soq1* with mutants impaired in specific carotenoids accumulation: *npq1* (lacks most zeaxanthin, Zea), *npq2* (lacks violaxanthin, Vx), *lut2* (lacks lutein) (16, 17), energy dissipation in the qH mechanism does not seem to require these pigments. However, in the *npq1* mutant there is a small pool of zeaxanthin as an intermediate in the conversion of ß-carotene to antheraxanthin and Vx (35), so we cannot totally exclude the possibility that qH requires zeaxanthin. However, the absence of CT or EET signals from carotenoids using transient absorption spectroscopy on thylakoids with qH ON further indicates that qH quenching may not involve a Chl-Car dissipative mechanism. In light of the absence of CT and EET signals, another possible path for energy dissipation could occur through Chl molecules via the so-called "Chl-concentration quenching" phenomenon. The concentration of Chl in the chloroplast is in the range of 10^{-1} M, yet the antenna fluoresces, whereas from a solution of 10^{-3} M Chl there is no fluorescence signal due to self-quenching (36). In proteins, Chls are bound to prevent self-quenching, such that they are "close but not too close" to enable light harvesting (37). Assuming that we cannot observe the CT and EET signals due to competition with another quenching mechanism, qH could be due to Chl-concentration quenching occurring in the LHCII trimer (Fig. 5).

Miloslavina et al. (29) have shown that oligomers or aggregates of LHCII trimers have mixed Chl-Chl excited and charge transfer states emitting in the far-red region of the spectrum and that zeaxanthin is not required but enhances this phenomenon. We have not detected this signal (Fig. S10) and could not fit the decays with a fixed lifetime component at 400 ps, as it is too long to fit the fluorescence decays in *soq1 roqh1* displaying constitutive qH with τ_{avg} of 105 or 126 ps (Table S2). This short τ_{avg} value was unchanged whether we selectively excited chlorophyll *a* or *b* (Fig. S10) and was similarly short across detection wavelengths ranging from 640 to 780 nm with shortest lifetime between 660-690 nm, the emission region associated with LHCII, and the PSI emission was shifted towards 720 nm instead of 740 nm when normalized with wild type to their respective maxima (Fig. S11). These results are indicative of a strong LHCII antenna quenching of both PSII-LHCII and possibly PSI-LHCI fluorescence (and/or PSI amount may also be lower). A decay associated spectra analysis was unsuccessful, because we could not fit both wild type and *soq1 roqh1* properly (depending on which time component we constrain, it was either too long for *soq1 roqh1* or too short for wild type). A model including τ_{avg} and spectral information could be created (see for a recent example (38) to test whether quenching of PSII is due to energy transfer at PSI (through charge separation from P_{700} or thermal dissipation by P_{700}^{+}), a process referred to as spillover, or quenching at both PSII and PSI is due to thermal dissipation at LHCII. Although we cannot investigate the fluorescence decays as early as ~5 ps due to the longer (30-40 ps) instrument response function (IRF), we observed that the normalized fluorescence decays of wild type and *soq1 roqh1* at 710 nm are almost the same before 100 ps (Fig. S12), suggesting that there is no major contribution of PSII to PSI spillover (within the time-resolution of the IRF).

It is possible that qH stems from a pure Chl-Chl CT state, which is not visible as a far-red emission, because it involves symmetry-breaking charge transfer and very rapid recombination to the ground state (39). Furthermore, because excited Chl has a broad spectrum due to a large number of energy transition states, no clean peak can be observed as is the case for violaxanthin or zeaxanthin. A small change in the conformation of the antenna modifying the protein environment of Chls or their orientation and/or distance with each other could enable qH, and identifying this fine-tuning will be the subject of future investigations. Such a structural switch has been proposed previously for qE (1).

Less qH in isolated system compared to intact ones

We observed that the average fluorescence lifetimes from thylakoids and isolated trimers are shorter when qH is ON but to a lesser extent than in leaves, and isolated trimers display the least difference among these three type of samples (*soq1*, Fig. 2 and 5 vs. Fig. 1, red bars). It is possible that the qH response observed *in vivo* is due to specific lipid-protein or protein-protein interactions that are altered upon thylakoid extraction and solubilization or that qH relaxes slowly during isolation of thylakoids or photosynthetic complexes. The difference in average fluorescence lifetimes could also be explained by altered connectivity between the antenna proteins in isolated systems as indicated by the step solubilization of thylakoids (Fig. S2). It has previously been observed that LH1 and LH2 antenna rings in purple bacteria for example displayed a 50% shorter lifetime *in vivo* compared to *in vitro* (40). Lifetimes of pigment-protein complexes largely depend on their local environment, e.g. detergent or proteoliposome (41-43). The density of the micelles containing the LHCII trimers is similar with qH ON/OFF based on their respective peaks overlaying each other after separation by gel filtration (Fig. S3). It is possible that the trimer fraction contains micelles with one LHCII trimer only and others with one LHCII trimer plus one monomer (consisting of either a major or minor Lhcb). We checked the content of these fractions by immunoblot as a different amount of Lhcb4 could have explained the difference in fluorescence lifetime (44) and found that the protein content was similar with qH ON or OFF and specifically that the amount of minor antenna Lhcb4 was similarly low (Fig. S5B and S8). Additionally, we observed quenching in the LHCII trimer by CN-PAGE (Fig. 4) shown to solely contain Lhcb1, 2 and 3 (45). Furthermore, there could be a mixed population of trimers, with some having qH ON or OFF, and this would become more evident once isolated (assuming connectivity between trimers is required for full quenching); the resulting average lifetime being an average of an ensemble of LHCII trimers with varying degrees of qH ON and OFF. Using single molecule spectroscopy, we will test whether the LHCII trimer fraction consists of a few trimers highly quenched or all trimers moderately quenched. For qE, it has been modeled that 12% of sites with active NPQ are sufficient to explain wild-type levels of NPQ (46).

Location of qH is likely in the LHCII trimer

Decreased fluorescence lifetimes of isolated LHCII trimer fractions with qH ON indicate that qH likely occurs in the trimer (Fig. 4, 5). Through genetic crosses, we found that qH does not require a specific Lhcb subunit of LHCII (Fig. 6), but it may rather require the trimeric conformation as monomerized LHCII and minor antenna proteins have similar fluorescence lifetimes whether qH ON or OFF (Fig. 5). LHCII can form homo-trimers of Lhcb1 or Lhcb2 or hetero-trimers composed of Lhcb1, Lhcb2, and/or Lhcb3 (47). Lhcb1 is the most abundant isoform representing roughly 70% of the total LHCII proteins, whereas Lhcb2 and Lhcb3 abundance is about 20% and 10%, respectively (47). LHCII proteins are highly conserved with an amino acid identity of 82% between Lhcb1 and Lhcb2, 78% between Lhcb1 and Lhcb3, and 79% between Lhcb2 and Lhcb3 (48). When a specific major Lhcb is missing, other major or minor Lhcb proteins are upregulated and can occupy the place of the missing Lhcb in the trimer, therefore qH may be insensitive to the subunit composition of the trimer. Indeed, when all genes of *LHCB1,* or *LHCB2,* are knocked down, an increase in Lhcb2 and Lhcb3, or Lhcb3 and Lhcb5 respectively, is observed (49) (however, when all *LHCB1* and *LHCB2* genes are knocked-down, Lhcb5 is not upregulated (50)). Finally, when *LHCB3* is knocked out, an increase of Lhcb1 and Lhcb2 is observed (51). Thus, in a major *lhcb* mutant, the antenna complexes are not completely disrupted, and compensation occurs. If qH requires Lhcb trimeric conformation irrespective of its composition, we expect no changes or only slight changes in qH induction in the *soq1 lhcb1*, *2*, or *3* mutants as we have found (Fig. 6).

Here, we have characterized the Chl fluorescence lifetime of intact leaves, thylakoids, and isolated antenna complexes with qH ON or OFF. We have observed quenching in all qH ON samples with a larger extent *in vivo*, highlighting the possible need of a preserved thylakoid membrane macroorganisation for a full qH response. Of note, the LHCII trimer fraction displayed qH whereas the monomer fraction did not, and qH does not rely on a specific major Lhcb protein. The photophysical mechanism of qH does not appear to involve CT or EET to a Car as no Car cation radical or S_1 excited states were observed. Another possible mechanism could involve Chl-Chl charge transfer, which due to its rapid nature cannot be spectroscopically observed. In future work, we will identify the structural changes in LHCII trimers with qH ON, monitor by single molecule spectroscopy the homogeneity of the qH response among LHCII trimers, and test its requirement for trimerization and/or connection to the core of PSII.

Materials and Methods

Plant material and growth conditions

Wild-type *Arabidopsis thaliana* and derived mutants studied here are of Col-0 ecotype. Mutants from these respective studies were used: *soq1* (16), *soq1 lcnp* (17), *roqh1-1*, *-2*, *-3*, *soq1 roqh1-1*, *-2*, *-3*, *soq1 roqh1 ROQH1 OE*, *soq1 roqh1 lcnp*, *soq1 npq4 roqh1* (18), *lhcb3* (SALK_036200C) (52). For clarity, we refer to the *lhcb1* quintuple mutant affected in all five *LHCB1* genes as "*lhcb1*" (CRISPR-Cas9 edits for *lhcb1.1* (nucleotide insertion (nt) 575_576insA), *lhcb1.2* (nt deletion 575del), *lhcb1.3* (nt insertion 419_420insT), *lhcb1.4* (nt insertion 416_417insT), *lhcb1.5* (large deletion 413_581del)) and to the *lhcb2* triple mutant affected in all three *LHCB2* genes as "*lhcb2"* (*lhcb2.1* (SALK_005774C), CRISPR-Cas9 edits for *lhcb2.2* (nt insertion 10insA), *lhcb2.3* (nt insertion 93insA)). Mutants *soq1 lhcb1*, *soq1 lhcb2* and *soq1 lhcb3* were generated in this study. Plants were grown on soil (Sunshine Mix 4/LA4 potting mix, Sun Gro Horticulture Distribution (Berkeley), 1:3 mixture of Agra-vermiculite "yrkeskvalité K-JORD" provided by RHP and Hasselfors garden respectively (Umeå)) under a 10/14h light/dark photoperiod at 120 µmol photons m^{-2} s^{-1} at 21°C (Berkeley) or 8/16h at 150 µmol photons m^{-2} s^{-1} at 22 °C/18°C (Umeå) for 5 to 6 weeks or seeds were surface sterilized using 70% ethanol and sown on agar plates (0.5 x Murashige and Skoog Basal Salt Mixture, Duchefa Biochemie, with pH adjusted to 5.7 with KOH) placed for 1 day in the dark at 4 °C, grown for 3 weeks with 12/12h at 150 µmol photons m^{-2} s^{-1} at 22°C and then transferred to soil. For the cold and high light treatment, plants or detached leaves were placed for 6h at 6°C and at 1500 µmol photons m^{-2} s^{-1} using a custom-designed LED panel built by JBeamBio with cool white LEDs BXRA-56C1100-B-00 (Farnell). Light bulbs used in growth chambers are cool white (4100K) from Philips (F25T8/TL841 25W) for plants grown on soil and from General Electric (F17T8/SP41 17W) for seedlings grown on agar plates.

Genetic crosses and genotyping primers

Genetic crosses were done using standard techniques (53). Phire Plant Direct PCR kit was used for genotyping with dilution protocol (ThermoFisher Scientific F130), primer list can be found in Table S3.

Chlorophyll fluorescence imaging

Chlorophyll fluorescence was measured at room temperature with Walz Imaging-PAM Maxi (Fig. S3, S4) or with SpeedZenII from JbeamBio (Fig. 4, 6). For NPQ measurements, plants or detached leaves were dark-acclimated for 20 min and NPQ was induced by 1200 µmol photons m^{-2} s^{-1} for 10 min and relaxed in the dark for 10 min. Maximum fluorescence after dark acclimation (F_m) and throughout measurement (F_m') were recorded after applying a saturating pulse of light. NPQ was calculated as (F_m-F_m')/F_m'. F_v/F_m is calculated as (F_m-F_o)/F_m where F_o is the minimum fluorescence after dark acclimation.

Thylakoid extraction

Thylakoid extractions were performed according to (54). Briefly, leaves from 6 to 8-week-old plants were ground in a blender for 30 s in 60 mL B1 cold solution (20 mM Tricine-KOH pH7.8, 400 mM NaCl, 2 mM $MgCl_2$). Protease inhibitors are used at all steps (0.2 mM benzamidine, 1 mM aminocaproic acid, 0.2 mM PMSF). The solution is then filtrated through four layers of Miracloth and centrifuged 5 minutes at 27,000 x g at 4°C. The supernatant is discarded, and the pellet is resuspended in 15 mL B2 solution (20 mM Tricine-KOH pH 7.8, 150 mM NaCl, 5 mM $MgCl_2$). The resuspended solution is overlayed onto a 1.3 M/1.8 M sucrose cushion and ultracentrifuged for 30 min in a SW28 rotor at 131,500 x g and 4°C. The band between the sucrose layers is removed and washed with B3 solution (20 mM Tricine-KOH pH 7.8, 15 mM NaCl, 5 mM $MgCl_2$). The solution is centrifuged for 15 min at 27,000 x g and 4°C. The pellet is washed in storing solution (20 mM Tricine-KOH pH 7.8, 0.4 M sucrose, 15 mM NaCl, 5 mM $MgCl_2$) and centrifuged for 10 min at 27,000 x g and 4°C. The pellet is then resuspended in storing solution. Chlorophyll concentration is measured according to (55). If samples are to be stored, they were flash-frozen in liquid nitrogen and stored at -80°C at approximately 2.5 mg Chl mL^{-1}. Upon using thylakoid preparation, samples are rapidly thawed and buffer is exchanged with 120 mM Tris-HCl pH 6.8, and chlorophyll concentration is measured. For spectroscopy experiments, thylakoids were isolated according to (56). For the 'before treatment' or 'dark' condition, leaves were detached and dark-acclimated overnight at 4°C.

Isolation of pigment-protein complexes

Thylakoids membranes (400 µg Chl) were solubilized at 2 mg mL^{-1} with 4% (w/v) α-dodecyl maltoside (α-DM) for 15 min on ice (solution was briefly mixed every 5 min), unsolubilized membranes were removed by centrifugation at 14,000 rpm for 5 min. Gel filtration chromatography was performed as described in (54) using the ÄKTAmicro chromatography system with a Superdex 200 Increase 10/300 GL column (GE Healthcare) equilibrated with 20 mM Tris-HCl (pH 8.0), 5 mM $MgCl_2$ and 0.03% (wt/vol) α-DM at room temperature. The flow rate was 1 mL min^{-1}. The proteins were detected at 280 nm absorbance.

Protein analysis

A 5 mm diameter disc was cut from the leaf and frozen into liquid nitrogen. The leaf disc was ground with a plastic pestle and 100 µL of sample loading buffer (62.5 mM Tris pH7.5, 2% SDS, 10% Glycerol, 0.01% Bromophenol blue, 100mM DTT) was added. Samples were boiled at 95-100°C for 5 min and centrifuged for 3 min. From the samples, 10 µL were loaded onto a 10% SDS-PAGE gel. For the gel filtration fractions, samples were loaded at same volume from pooled adjacent fractions (three fractions for each) onto a 12% SDS-PAGE gel for immunoblot or for silver stain. After migration the proteins were transferred to a PVDF 0.45 µm from ThermoScientific. After transferring the membrane was blocked with TBST+ 3% milk for 1h followed by 1h incubation of the primary antibody (ATP*b* AS05 085, LHCB1 AS09 522, LHCB2 AS01 003, LHCB3 AS01 002, LHCB4 AS04 045 from Agrisera) diluted in TBST+ 3% milk. The membrane was washed 3 times 10 min with TBST. Then incubated for 1h with the secondary antibody conjugated to horse radish peroxidase (AS09 602 from Agrisera) in TBST + 3% milk. The membrane was washed 3 times 10 min with TBST and 1 time 5 min with TBS. The Agrisera ECL Bright (AS16 ECL-N-100) and Azure biosystems c600 were used to reveal the bands.

Clear-native PAGE analysis

Thylakoid are washed with the solubilization buffer (25 mM BisTris/HCl (pH 7.0), 20% (w/v) glycerol, 1mM *ε*-aminocaproic acid and 0.2 mM PMSF) and resuspended in the same buffer at 1 mg Chl mL^{-1}. An equal volume of 2% α-DM was added to the thylakoid solution for 15 min on ice in the dark. Traces of insoluble material were removed by centrifugation at 18,000 x g 20 min 4°C.

The chlorophyll concentration was measured, and proteins were loaded at equal chlorophyll content in the native gel (NativePAGE™ 3 to 12%, Bis-Tris, 1.0 mm, Mini Protein Gel, 10-well from ThermoFisher catalog number BN1001BOX). Prior to loading the samples were supplemented with sodium deoxycholate (final concentration 0.3%). The cathode buffer is 50 mM Tricine, 15 mM BisTris, 0.05% sodium deoxycholate and 0.02% α-DM, pH7.0 and anode buffer is 50 mM BisTris, pH7.0. Electrophoresis was performed at 4°C with a gradual increase in voltage: 75 V for 30 min, 100 V for 30 min, 125 V for 30 min, 150 V for 1 h and 175 V until the sample reached the end of the gel. Method adapted from (57).

Pigment extraction and analysis

HPLC analysis of carotenoids and chlorophylls was done as previously described (58). 10 µg Chl of fraction samples were extracted in 200 µl 100% acetone.

Fluorescence spectroscopy on isolated thylakoids or complexes

Room temperature fluorescence emission of gel filtration fractions and dependence on step solubilization of thylakoids were performed according to (14) using a Horiba FluoroMax fluorimeter and Starna cells 18/9F-SOG-10 (path length 10mm) with chlorophyll concentration of 0.1 µg mL^{-1}. For the emission spectrum of gel filtration fractions (emission 650 to 800 nm with excitation at 625 nm, bandwidth, 5 nm for excitation, 5 nm for emission), samples were diluted at same absorption (Δ625-750 nm=0.0005) in 20 mM Tris HCl pH8, 5 mM $MgCl_2$ and 0.03% α-DM. For the step solubilization (emission 680 nm with excitation at 440 nm, bandwidth, 5 nm for excitation, 3 nm for emission), thylakoids preparation were diluted in 20 mM Tris HCl pH8, 5 mM $MgCl_2$, and two different detergents were added: first, α-DM at final 0.5% (w/v) concentration from a 10% stock solution, then Triton X-100 at final 5% (w/v) concentration from a 50% stock solution. After each addition, the cuvette was turned upside-down 3 to 5 times for mixing and time for fluorescence level stabilization was allowed.

Fluorescence lifetime and transient absorption spectroscopy snapshot

Method used is adapted for fluorescence lifetime snapshot from (59) and transient absorption spectroscopy snapshot from (60). For fluorescence lifetime measurements, time-correlated single

photon counting (TCSPC) was performed on detached leaves, isolated thylakoids and gel filtration fractions. Excitation at 420 nm was provided by frequency doubling the output of a Ti:sapphire oscillator (Coherent, Mira 900f, 76 MHz). The laser intensity was ~1800 µmol photons m^{-2} s^{-1}/pulse (~10 pJ/pulse). Emission was monitored at 680 nm using a MCP PMT detector (Hamamatsu, R3809U). The FWHM of IRF was ~30-40 ps. Fluorescence decays were fitted with 3 exponential decay components (Picoquant, Fluofit Pro-4.6). qE is relaxed by dark-acclimation for at least 5 min before each measurement. Transient absorption (TA) spectroscopy was performed on isolated thylakoids at 80 µg Chl mL^{-1}. Experimental details of the apparatus were as in (27) for the CT mechanism and (22) for the EET mechanism.

Accession Numbers

Sequence data from this article can be found in the Arabidopsis Genome Initiative under accession numbers At1g29920 (LHCB1.1), At1g29910 (LHCB1.2), At1g29930 (LHCB1.3), At1g56500 (SOQ1), At2g05070 (LHCB2.2), At2g05100 (LHCB2.1), At2g34420 (LHCB1.5), At2g34430 (LHCB1.4), At3g27690 (LHCB2.3), At3g47860 (LCNP), At4g31530 (ROQH1), At5g54270 (LHCB3).

Author Contributions: A.M., K.K.N. and G.R.F. designed research; A.M., S.P., C.J.S., E.J.S.-G., C.L.A., M.L. and L.L. performed biochemical isolation and spectroscopy and analyzed the data; F.L. generated the *lhcb1* and *lhcb2* lines; P.B. performed crosses and analyses of *lhcb* mutants. All of the authors discussed the data, and A.M. wrote the paper with input from P.B., C.J.S., G.R.F and K.K.N.

Acknowledgments

We thank Masakazu Iwai for advice and technical assistance regarding isolation of pigment-protein complexes and for critical reading of the manuscript; Alexandra Lee Fisher for technical assistance with transient absorption spectroscopy experiments and Julie Guerreiro for assistance with antenna mutant combination analysis; Roberta Croce and Roberto Bassi for critical discussions. This research (Berkeley) was supported by the Division of Chemical Sciences, Geosciences and Biosciences, Office of Basic Energy Sciences, Office of Science, US Department of Energy (Field

Work Proposal 449B). K.K.N. is an investigator of the Howard Hughes Medical Institute. A.M. (Umeå) was supported by European Commission Marie Skłodowska-Curie Actions Individual Fellowship Reintegration Panel (845687). The research performed at Umeå (P.B. and A.M.) was supported by grants to UPSC from the Knut and Alice Wallenberg Foundation (2016.0341 and 2016.0352), the Swedish Governmental Agency for Innovation Systems (2016-00504), by a starting grant to A.M. from the Swedish Research Council Vetenskapsrådet (2018-04150) and by a consortium grant from the Swedish Foundation for Strategic Research (ARC19-0051). The research performed at Neuchâtel (F.L.) was supported by the Swiss National Science Foundation (31003A_179417).

Competing Interest Statement: The authors declare no conflict of interest.

Supplemental Data: Fig.S1 to S12 and Table S1 to S3.

References

1. N. Liguori, X. Periole, S. J. Marrink, R. Croce, From light-harvesting to photoprotection: structural basis of the dynamic switch of the major antenna complex of plants (LHCII). *Sci Rep* **5**, 15661 (2015).
2. L. Valkunas, J. Chmeliov, T. P. J. Krüger, C. Ilioaia, R. van Grondelle, How Photosynthetic Proteins Switch. *The Journal of Physical Chemistry Letters* **3**, 2779-2784 (2012).
3. X. G. Zhu, S. P. Long, D. R. Ort, Improving photosynthetic efficiency for greater yield. *Annu Rev Plant Biol* **61**, 235-261 (2010).
4. B. Demmig-Adams, G. Garab, W. Adams III, U. o. I. Govindjee, "Non-photochemical quenching and energy dissipation in plants, algae and cyanobacteria". (Springer, 2014), vol. 40.
5. Y. Wang, S. J. Burgess, E. M. de Becker, S. P. Long, Photosynthesis in the fleeting shadows: an overlooked opportunity for increasing crop productivity? *Plant J* **101**, 874-884 (2020).
6. J. Kromdijk *et al.*, Improving photosynthesis and crop productivity by accelerating recovery from photoprotection. *Science* **354**, 857-861 (2016).
7. D. R. Ort *et al.*, Redesigning photosynthesis to sustainably meet global food and bioenergy demand. *Proc Natl Acad Sci U S A* **112**, 8529-8536 (2015).
8. P. Horton, A. V. Ruban, R. G. Walters, Regulation of Light Harvesting in Green Plants. *Annu Rev Plant Physiol Plant Mol Biol* **47**, 655-684 (1996).
9. P. Müller, X. P. Li, K. K. Niyogi, Non-photochemical quenching. A response to excess light energy. *Plant Physiol* **125**, 1558-1566 (2001).

10. A. Pinnola, R. Bassi, Molecular mechanisms involved in plant photoprotection. *Biochem Soc Trans* **46**, 467-482 (2018).
11. A. Malnoë, Photoinhibition or photoprotection of photosynthesis? Update on the (newly termed) sustained quenching component, qH. *Environmental and Experimental Botany* **154**, 123-133 (2018).
12. R. Bassi, L. Dall'Osto, Dissipation of Light Energy Absorbed in Excess: The Molecular Mechanisms. *Annu Rev Plant Biol* **72**, 47-76 (2021).
13. K. K. Niyogi, T. B. Truong, Evolution of flexible non-photochemical quenching mechanisms that regulate light harvesting in oxygenic photosynthesis. *Curr Opin Plant Biol* **16**, 307-314 (2013).
14. L. Dall'Osto, S. Caffarri, R. Bassi, A mechanism of nonphotochemical energy dissipation, independent from PsbS, revealed by a conformational change in the antenna protein CP26. *Plant Cell* **17**, 1217-1232 (2005).
15. G. H. Krause, S. Somersalo, E. Zumbusch, B. Weyers, H. Laasch, On the Mechanism of Photoinhibition in Chloroplasts. Relationship Between Changes in Fluorescence and Activity of Photosystem II. *Journal of Plant Physiology* **136**, 472-479 (1990).
16. M. D. Brooks, E. J. Sylak-Glassman, G. R. Fleming, K. K. Niyogi, A thioredoxin-like/beta-propeller protein maintains the efficiency of light harvesting in *Arabidopsis*. *Proc Natl Acad Sci USA* **110**, 2733-2740 (2013).
17. A. Malnoë *et al.*, The Plastid Lipocalin LCNP Is Required for Sustained Photoprotective Energy Dissipation in Arabidopsis. *Plant Cell* **30**, 196-208 (2018).
18. C. L. Amstutz *et al.*, An atypical short-chain dehydrogenase-reductase functions in the relaxation of photoprotective qH in Arabidopsis. *Nat Plants* **6**, 154-166 (2020).
19. P. Bru, S. Nanda, A. Malnoë, A Genetic Screen to Identify New Molecular Players Involved in Photoprotection qH in Arabidopsis thaliana. *Plants* **9**, 1565 (2020).
20. G. Levesque-Tremblay, M. Havaux, F. Ouellet, The chloroplastic lipocalin AtCHL prevents lipid peroxidation and protects *Arabidopsis* against oxidative stress. *Plant J* **60**, 691-702 (2009).
21. Y. Z. Ma, N. E. Holt, X. P. Li, K. K. Niyogi, G. R. Fleming, Evidence for direct carotenoid involvement in the regulation of photosynthetic light harvesting. *Proc Natl Acad Sci U S A* **100**, 4377-4382 (2003).
22. S. Park *et al.*, Chlorophyll-Carotenoid Excitation Energy Transfer in High-Light-Exposed Thylakoid Membranes Investigated by Snapshot Transient Absorption Spectroscopy. *J Am Chem Soc* **140**, 11965-11973 (2018).
23. N. Liguori *et al.*, Different carotenoid conformations have distinct functions in light-harvesting regulation in plants. *Nat Commun* **8**, 1994 (2017).
24. M. Son, A. Pinnola, S. C. Gordon, R. Bassi, G. S. Schlau-Cohen, Observation of dissipative chlorophyll-to-carotenoid energy transfer in light-harvesting complex II in membrane nanodiscs. *Nat Commun* **11**, 1295 (2020).
25. A. Pinnola *et al.*, Electron transfer between carotenoid and chlorophyll contributes to quenching in the LHCSR1 protein from Physcomitrella patens. *Biochim Biophys Acta* **1857**, 1870-1878 (2016).
26. N. E. Holt *et al.*, Carotenoid cation formation and the regulation of photosynthetic light harvesting. *Science* **307**, 433-436 (2005).

27. S. Park *et al.*, Snapshot Transient Absorption Spectroscopy of Carotenoid Radical Cations in High-Light-Acclimating Thylakoid Membranes. *J Phys Chem Lett* **8**, 5548-5554 (2017).
28. L. Cupellini, D. Calvani, D. Jacquemin, B. Mennucci, Charge transfer from the carotenoid can quench chlorophyll excitation in antenna complexes of plants. *Nat Commun* **11**, 662 (2020).
29. Y. Miloslavina *et al.*, Far-red fluorescence: a direct spectroscopic marker for LHCII oligomer formation in non-photochemical quenching. *FEBS Lett* **582**, 3625-3631 (2008).
30. D. I. G. Bennett *et al.*, Models and mechanisms of the rapidly reversible regulation of photosynthetic light harvesting. *Open Biol* **9**, 190043 (2019).
31. M. Ballottari, J. Girardon, L. Dall'osto, R. Bassi, Evolution and functional properties of photosystem II light harvesting complexes in eukaryotes. *Biochim Biophys Acta* **1817**, 143-157 (2012).
32. A. Crepin, S. Caffarri, Functions and Evolution of Lhcb Isoforms Composing LHCII, the Major Light Harvesting Complex of Photosystem II of Green Eukaryotic Organisms. *Curr Protein Pept Sci* **19**, 699-713 (2018).
33. P. Jahns, A. R. Holzwarth, The role of the xanthophyll cycle and of lutein in photoprotection of photosystem II. *Biochim Biophys Acta* **1817**, 182-193 (2012).
34. E. J. Sylak-Glassman, J. Zaks, K. Amarnath, M. Leuenberger, G. R. Fleming, Characterizing non-photochemical quenching in leaves through fluorescence lifetime snapshots. *Photosynth Res* **127**, 69-76 (2016).
35. B. Demmig-Adams, J. J. Stewart, M. López-Pozo, S. K. Polutchko, W. W. Adams, Zeaxanthin, a Molecule for Photoprotection in Many Different Environments. *Molecules* **25**, 5825 (2020).
36. W. F. Watson, R. Livingston, Concentration quenching of fluorescence in chlorophyll solutions. *Nature* **162**, 452 (1948).
37. G. S. Beddard, G. Porter, Concentration quenching in chlorophyll. *Nature* **260**, 366-367 (1976).
38. P. Bag *et al.*, Direct energy transfer from photosystem II to photosystem I confers winter sustainability in Scots Pine. *Nat Commun* **11**, 6388 (2020).
39. M. Kellogg *et al.*, Symmetry breaking charge transfer as a means to study electron transfer with no driving force. *Faraday Discussions* **216**, 379-394 (2019).
40. M. Ricci, S. E. Bradforth, R. Jimenez, G. R. Fleming, Internal conversion and energy transfer dynamics of spheroidene in solution and in the LH-1 and LH-2 light-harvesting complexes. *Chemical Physics Letters* **259**, 381-390 (1996).
41. A. Crepin, E. Cunill-Semanat, E. Kuthanova Trskova, E. Belgio, R. Kana, Antenna Protein Clustering In Vitro Unveiled by Fluorescence Correlation Spectroscopy. *Int J Mol Sci* **22** (2021).
42. L. Nicol, R. Croce, The PsbS protein and low pH are necessary and sufficient to induce quenching in the light-harvesting complex of plants LHCII. *Sci Rep* **11**, 7415 (2021).
43. S. Tietz *et al.*, A proteoliposome-based system reveals how lipids control photosynthetic light harvesting. *J Biol Chem* **295**, 1857-1866 (2020).
44. P. Xu, L. Tian, M. Kloz, R. Croce, Molecular insights into zeaxanthin-dependent quenching in higher plants. *Sci Rep* **5**, 13679 (2015).
45. M. Rantala, V. Paakkarinen, E.-M. Aro, Separation of Thylakoid Protein Complexes with Two-dimensional Native-PAGE. *Bio-protocol* **8**, e2899 (2018).

46. D. I. G. Bennett, G. R. Fleming, K. Amarnath, Energy-dependent quenching adjusts the excitation diffusion length to regulate photosynthetic light harvesting. *Proc Natl Acad Sci U S A* **115**, E9523-E9531 (2018).
47. J. Standfuss, W. Kuhlbrandt, The three isoforms of the light-harvesting complex II: spectroscopic features, trimer formation, and functional roles. *J Biol Chem* **279**, 36884-36891 (2004).
48. S. Caffarri, R. Croce, L. Cattivelli, R. Bassi, A look within LHCII: differential analysis of the Lhcb1-3 complexes building the major trimeric antenna complex of higher-plant photosynthesis. *Biochemistry* **43**, 9467-9476 (2004).
49. M. Pietrzykowska *et al.*, The light-harvesting chlorophyll a/b binding proteins Lhcb1 and Lhcb2 play complementary roles during state transitions in Arabidopsis. *Plant Cell* **26**, 3646-3660 (2014).
50. L. Nicol, W. J. Nawrocki, R. Croce, Disentangling the sites of non-photochemical quenching in vascular plants. *Nat Plants* **5**, 1177-1183 (2019).
51. J. T. Damkjaer *et al.*, The photosystem II light-harvesting protein Lhcb3 affects the macrostructure of photosystem II and the rate of state transitions in Arabidopsis. *Plant Cell* **21**, 3245-3256 (2009).
52. Y.-H. Xu *et al.*, Light-harvesting chlorophyll a/b-binding proteins are required for stomatal response to abscisic acid in Arabidopsis. *Journal of experimental botany* **63**, 1095-1106 (2012).
53. D. Weigel, J. Glazebrook, Setting Up *Arabidopsis* Crosses. *Cold Spring Harbor Protocols* 10.1101/pdb.prot4623 (2006).
54. M. Iwai *et al.*, Light-harvesting complex Lhcb9 confers a green alga-type photosystem I supercomplex to the moss Physcomitrella patens. *Nat Plants* **1**, 14008 (2015).
55. R. J. Porra, W. A. Thompson, P. E. Kriedemann, Determination of accurate extinction coefficients and simultaneous equations for assaying chlorophylls a and b extracted with four different solvents: verification of the concentration of chlorophyll standards by atomic absorption spectroscopy. *Biochimica et Biophysica Acta (BBA) - Bioenergetics* **975**, 384-394 (1989).
56. A. M. Gilmore, V. P. Shinkarev, T. L. Hazlett, G. Govindjee, Quantitative analysis of the effects of intrathylakoid pH and xanthophyll cycle pigments on chlorophyll a fluorescence lifetime distributions and intensity in thylakoids. *Biochemistry* **37**, 13582-13593 (1998).
57. M. Rantala, V. Paakkarinen, E.-M. Aro, Analysis of Thylakoid Membrane Protein Complexes by Blue Native Gel Electrophoresis. *JoVE* doi:10.3791/58369, e58369 (2018).
58. P. Müller-Moulé, P. L. Conklin, K. K. Niyogi, Ascorbate deficiency can limit violaxanthin de-epoxidase activity *in vivo*. *Plant Physiol* **128**, 970-977 (2002).
59. C. J. Steen, J. M. Morris, A. H. Short, K. K. Niyogi, G. R. Fleming, Complex Roles of PsbS and Xanthophylls in the Regulation of Nonphotochemical Quenching in Arabidopsis thaliana under Fluctuating Light. *J Phys Chem B* **124**, 10311-10325 (2020).
60. S. Park, C. J. Steen, A. L. Fischer, G. R. Fleming, Snapshot transient absorption spectroscopy: toward in vivo investigations of nonphotochemical quenching mechanisms. *Photosynth Res* **141**, 367-376 (2019).

Figures

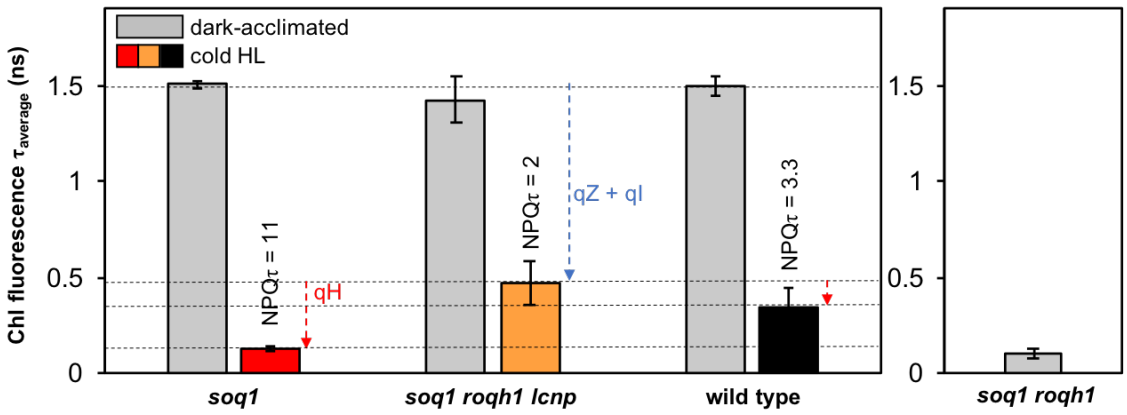

Figure 1. Fluorescence lifetime from leaves are shorter with qH ON.
Average fluorescence lifetime (τ_{avg}) of intact leaves before and after a cold and high-light (cold HL) treatment for 6h which induces qH in wild type and *soq1*. qE is relaxed by dark-acclimating for 5 min before each measurement. NPQτ values are determined based on: NPQτ = $\frac{\tau_{avg,\,dark} - \tau_{avg,light}}{\tau_{avg,light}}$. Data represent means ±SD (n=4 individuals before treatment, n=12 after cold HL treatment and n=17 *soq1 roqh1* no treatment). Excitation at 420 nm and emission at 680 nm.

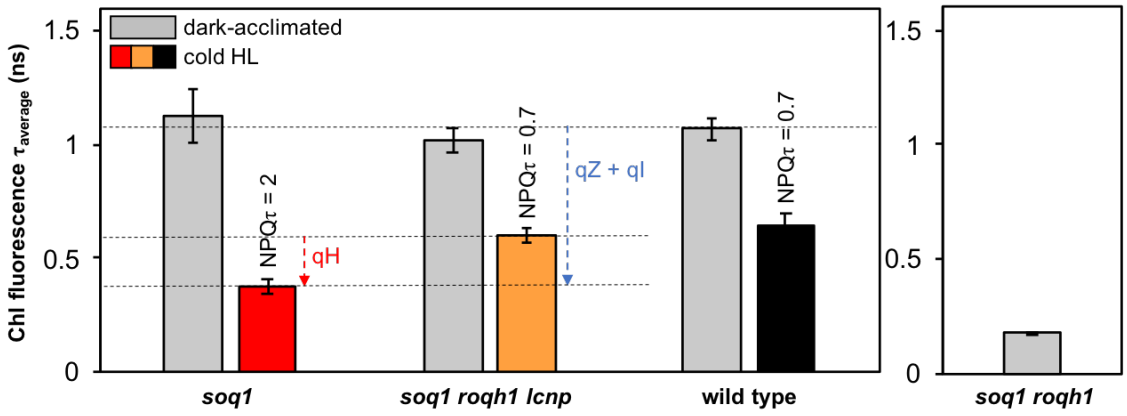

Figure 2. Fluorescence lifetime from isolated thylakoids are shorter with qH ON, but to a lesser extent than in leaves.
Average fluorescence lifetime ($\tau_{average}$) of crude thylakoid membrane isolated before (dark-acclimation overnight) and after a cold and high-light (cold HL) treatment for 6h which induces qH in wild type and *soq1*, qE is relaxed by dark-acclimating for 5 min before thylakoid isolation. Data represent means ±SD (n=3 technical replicates from 2 independent biological experiments).

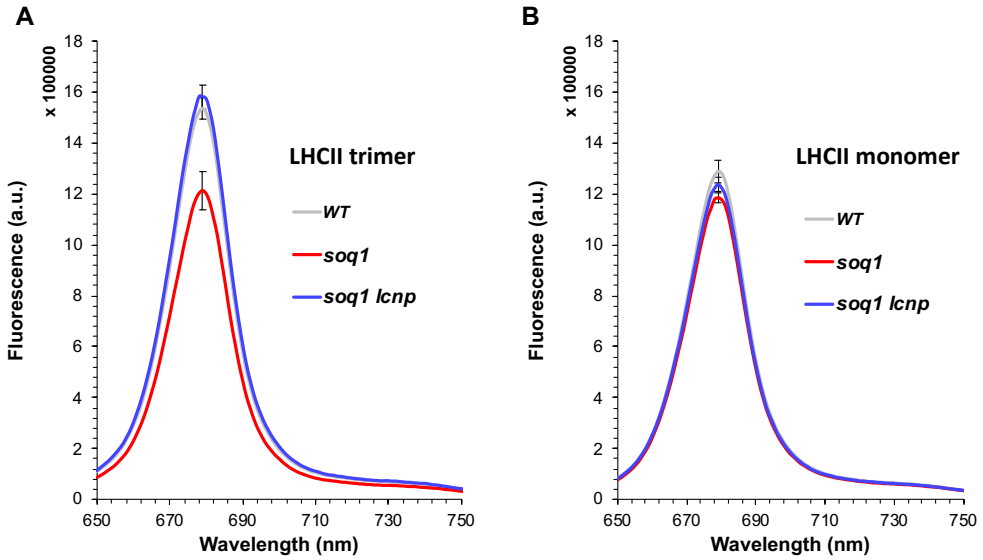

Figure 3. Fluorescence yield is ~20% lower with qH ON in LHCII trimer fraction only. Room temperature fluorescence spectra of isolated LHCII trimer (**A**) and LHCII monomer (**B**) pooled fractions from non-treated wild type (WT) (grey) and cold and HL-treated for 6h40 *soq1* (red) and *soq1 lcnp* (blue) (see Fig. S1 for representative gel filtration experiment and peaks annotation from which fractions were pooled). Fluorescence emission from 650 nm to 750 nm from samples diluted at same chlorophyll concentration (0.1 µg mL^{-1}) with excitation at 625 nm. Data represent means ±SD (n=3 technical replicates). Representative from three independent biological experiments is shown.

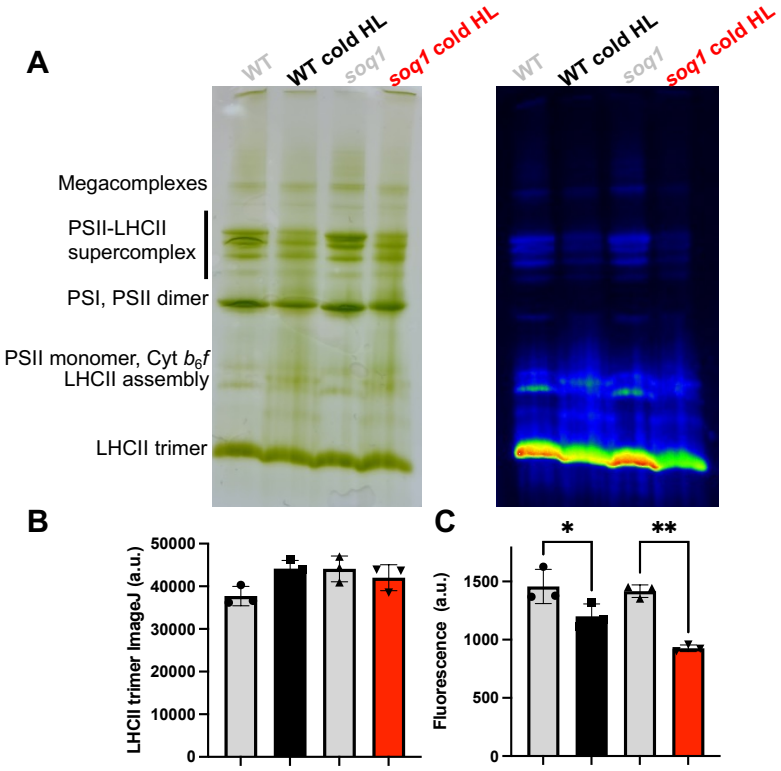

Figure 4. LHCII trimer band displays lower fluorescence when qH ON.
(**A**) Thylakoids were extracted from WT and *soq1* plants (n=3 individuals of each) grown under standard conditions (grey) or cold and high light (cold HL)-treated for 10h (black and red) with NPQ values of respectively 3±1 and 11±1, solubilized in 1% α-DM and separated by clear native PAGE on a 3-12% gel. 10 µg Chl were loaded per lane. Gel image (left) and chlorophyll fluorescence image (right). The composition of the major bands are indicated based on (Rantala *et al.* (2018)). (**B**) Scatter plot with bar representing the quantification of the LHCII trimer band shown in panel A using ImageJ. No statistical difference is measured between the samples. (**C**) Chlorophyll fluorescence quantification of the LHCII trimer band shown in panel A using SpeedZenII software from JBeamBio. Tukey's multiple comparisons test shows a significant decrease in fluorescence level between WT and WT cold HL **P*=0.0450 and between *soq1* and *soq1* cold HL ***P*=0.0011. (**B**,**C)** Data represent means of technical replicates ± SD (n=3 independent loaded gel lanes).

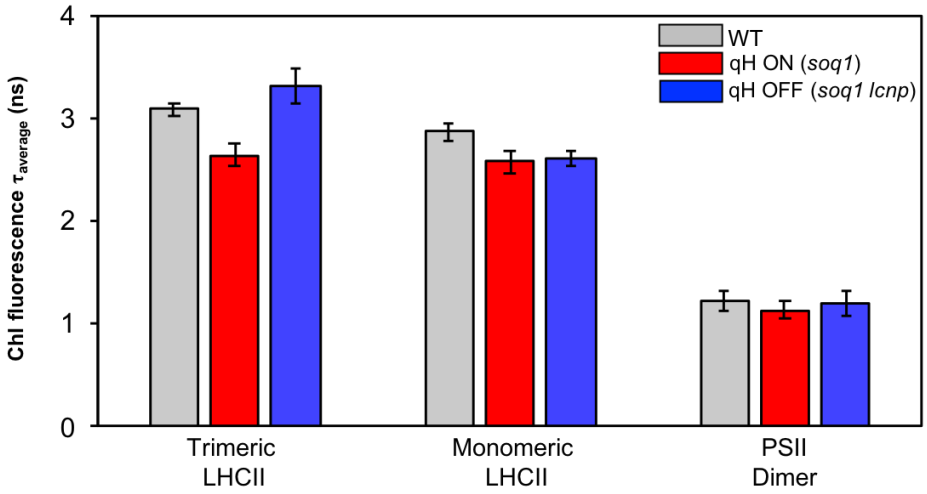

Figure 5. Fluorescence lifetime is 20% lower with qH ON in LHCII trimer fraction only.

Average fluorescence lifetime (τ_{avg}) of trimeric LHCII, monomeric LHCII, and PSII dimer isolated from non-treated wild type (WT) (grey) and cold HL-treated *soq1* (red) and *soq1 lcnp* (blue). Data represent means ±SD (n=3 technical replicates from 2 independent biological experiments).

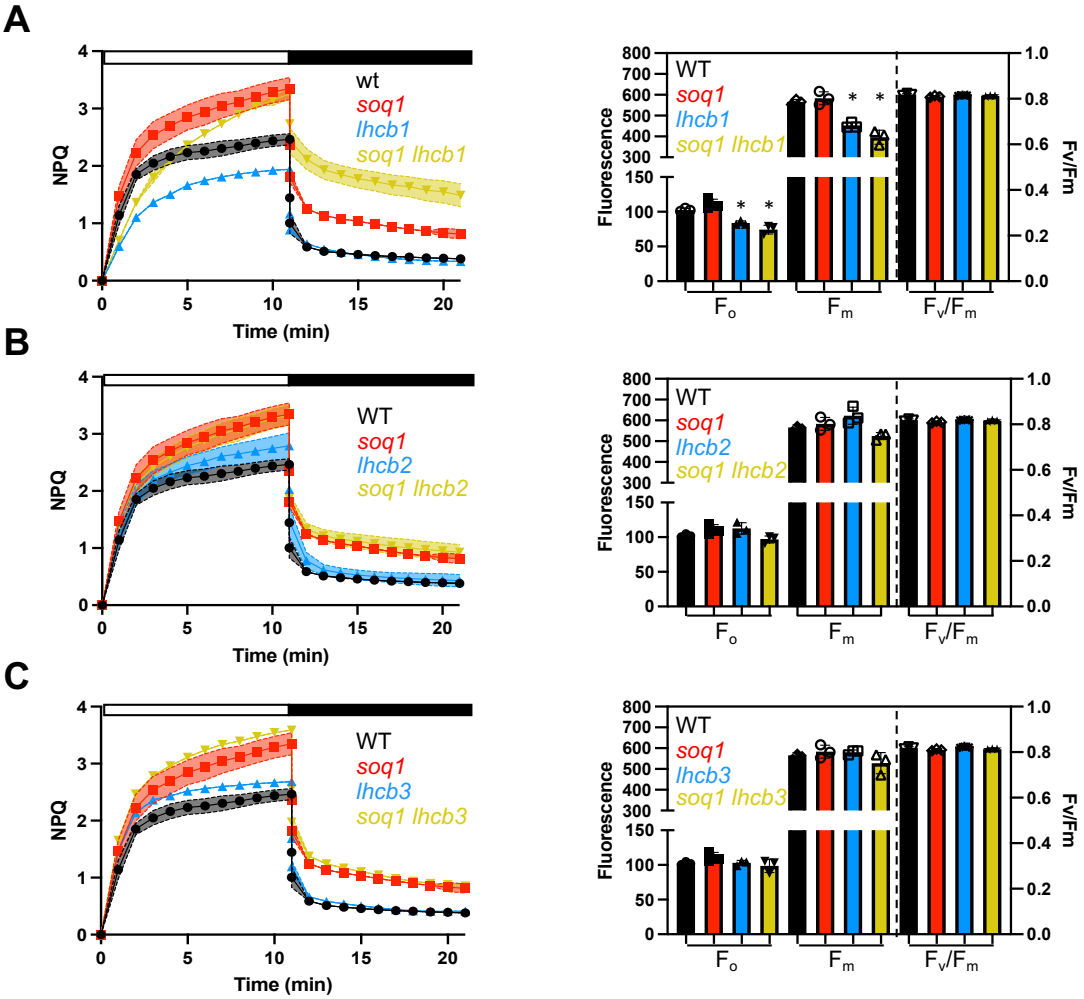

Figure 6. qH does not rely on a specific major Lhcb.
Left panel, NPQ kinetics of dark-acclimated (20 min) WT, *soq1*, (**A**) *lhcb1* and *soq1 lhcb1,* (**B**) *lhcb2* and *soq1 lhcb2,* (**C**) *lhcb3* and *soq1 lhcb3* four-week-old plants grown at 120 µmol photons m^{-2} s^{-1}. Induction of NPQ at 1300 µmol photons m^{-2} s^{-1} (white bar) and relaxation in the dark (black bar). Right panel, photosynthetic parameters F_o, F_m and F_v/F_m of the same plants. Tukey's multiple comparisons test shows that *lhcb1* and *soq1 lhcb1* are statistically different from WT for F_o (P=0.0096 and P=0.0008, respectively) and F_m (P=0.0023 and P=0.0001, respectively). Data represent means ± SD (n=3 individuals).

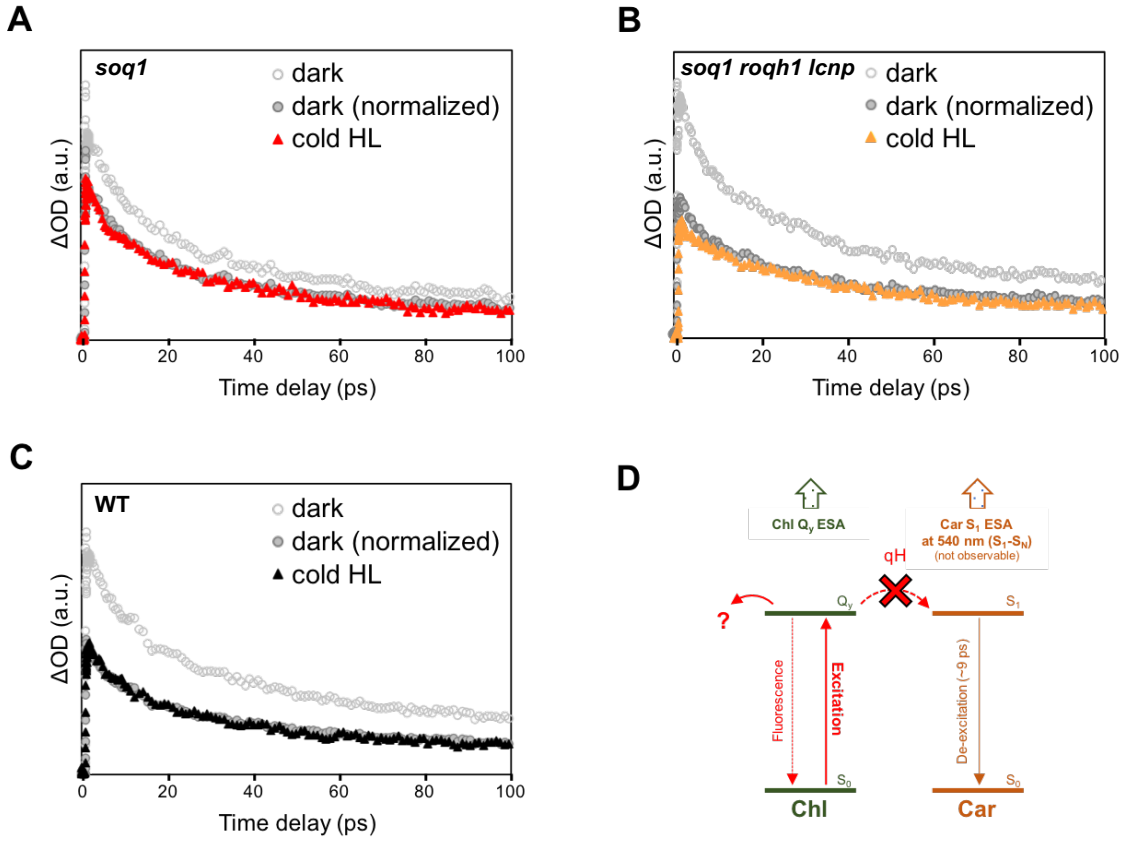

Figure 7. TA (Car S_1 excited state absorption at 540 nm) on thylakoid membranes. TA kinetic profiles for (A) *soq1*, (B) *soq1 roqh1 lcnp*, and (C) wild type Arabidopsis thylakoid membranes from leaves dark-acclimated overnight or after a cold HL treatment. The samples were excited and probed at 650 nm and 540 nm, respectively. Dark-adapted TA kinetics were normalized to match the respective kinetic measured from cold HL-treated sample. (D) Schematic illustration for Chl-Car excitation energy transfer mechanism for Chl* quenching, which could not be related to qH.

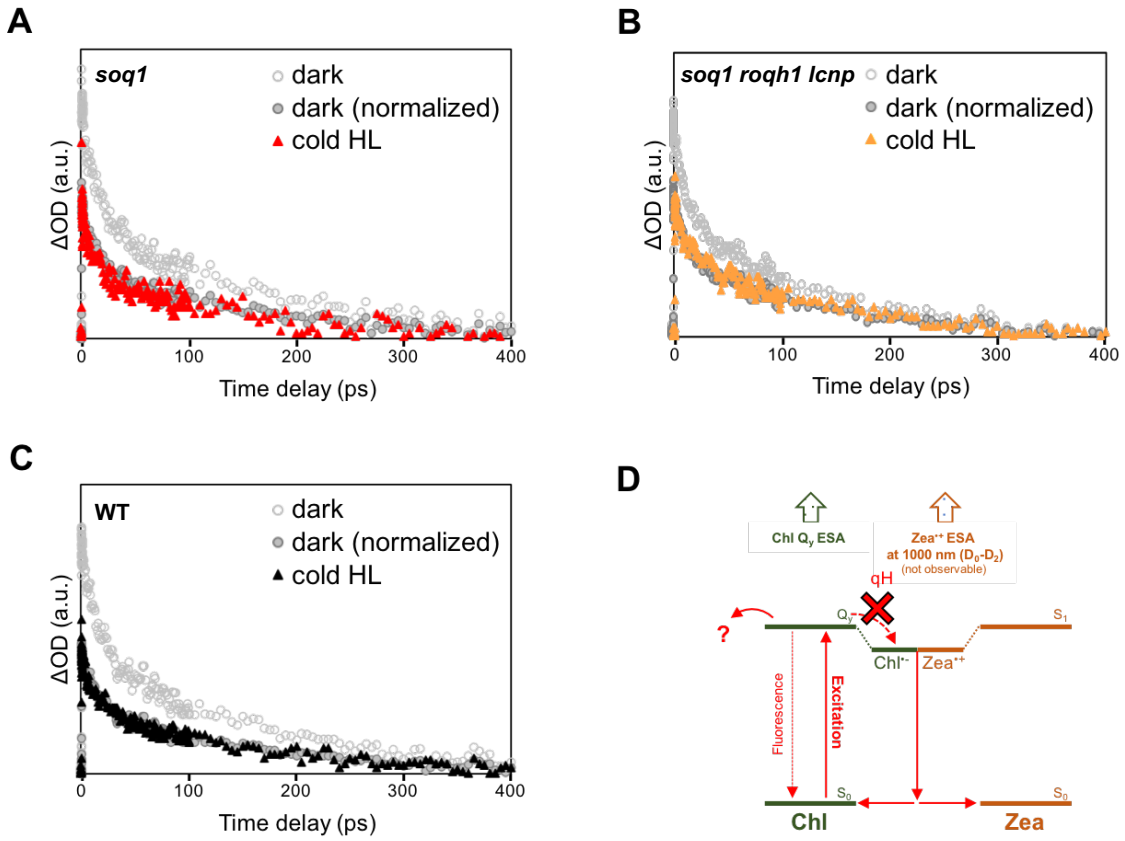

Figure 8. TA (Zea$^{\cdot+}$ excited state absorption at 1000 nm) on thylakoid membranes. TA kinetic profiles for (A) *soq1*, (B) *soq1 roqh1 lcnp*, and (C) wild type Arabidopsis thylakoid membranes isolated from leaves dark-acclimated overnight or after a cold HL treatment. The sample were excited and probed at 650 nm and 1000 nm, respectively. Dark-adapted TA kinetics were normalized to match the respective kinetic measured from cold HL-treated sample. (D) Schematic illustration for Chl-Car charge transfer mechanism for Chl* quenching, which could not be related to qH. (Lut$^{\cdot+}$ excited state absorption at 920 nm was also probed and no signal differences could be observed).